

# Effects of hot top pulsed magneto-oscillation on solidification structure of steel ingot

Hui-cheng Li<sup>1,2</sup>, Yu-xiang Liu<sup>1,2</sup>, \*Yun-hu Zhang<sup>1,2</sup>, Zhen Liu<sup>1,2</sup>, Qi-jie Zhai<sup>1,2,3</sup>

1. State Key Laboratory of Advanced Special Steels, Shanghai University, Shanghai 200072, China

2. School of Materials Science and Engineering, Shanghai University, Shanghai 200072, China

3. Materials Genome Institute, Shanghai University, Shanghai 200444, China.

**Abstract:** Achieving a uniform structure with few defects in heavy steel ingot is of high commercial importance. In this present work, in order to verify the potential of pulsed magneto-oscillation (PMO) applied in the production of heavy ingot, an induction coil was located at the hot top of the steel ingot to develop a novel technique, named hot top pulsed magneto oscillation (HPMO). The influences of HPMO on the solidification structure, macro segregation and compactness of a cylindrical medium carbon steel ingot with the weight of 160 kg were systematically investigated by optical microscope (OM) and laser induced breakdown spectroscopy original position metal analyzer (LIBSOPA-100). The results show that HPMO not only causes significant grain refinement and promotes the occurrence of columnar to equiaxed transition (CET) but also can homogenize the carbon distribution and enhance the compactness of the steel ingot. Therefore, HPMO technique has the potential to be applied in the production of heavy steel ingots on an industrial scale.

**Key words:** hot-top pulsed magneto oscillation (HPMO); solidified structures; defects of steel ingot

CLC numbers: TG142.11

Document code: A

Article ID: 1672-6421(2018)02-110-07

A sophisticated manufacturing process is frequently employed for large scale high performance parts. The process is usually as follows: a heavy ingot with a weight of more than 100 t is usually produced by mould casting, then the as-cast ingot is intensively forged and shaped, and eventually, heat treatment of the shaped part is applied to improve the final properties<sup>[1]</sup>. However, the final properties and quality of product are significantly deteriorated by the generated inherent defects in the heavy ingot, such as macro-segregation, inhomogeneous solidification structure, shrinkage, and so on<sup>[2-4]</sup>. Hence, decreasing these defects to improve the quality of product is of high commercial importance.

It has been recognized that the defects mentioned above can be reduced by improving the solidification process via optimizing the mould design, melting and pouring procedures<sup>[5,6]</sup>. In addition, the external energy fields have shown the prominent ability to improve the

solidified structures of alloys and reduce the proposed defects. For instance, it was reported that ultrasonic vibrations can lead to grain refinement, increase homogeneity and reduce segregation significantly<sup>[7,8]</sup>. Electromagnetic stirring (EMS) has been applied in continuous casting of steel to improve the solidification structure and reduce the segregation and porosity at industrial scale<sup>[9,10]</sup>. However, these two approaches are not suitable for the production of heavy ingots because the temperature of the steel melt is too high for the horn of ultrasonic vibration, and the geometry of the heavy ingot is too large for EMS.

Refining the microstructure is an effective method to homogenize macro segregation and decrease the shrinkage porosity, which is proved by many researchers<sup>[11-13]</sup>. Recently, the influence of pulsed electromagnetic fields on the solidification of metal alloys has been intensively investigated because it has shown a strong ability of refining grain significantly. For instance, Liao et al. studied the refined effect of electric current pulse (ECP) technology on the solidified structure of Al, and the result showed that the structure can be dramatically refined during nucleation<sup>[14]</sup>. Besides, the solidification experiment of high carbon steel ingot has been performed successfully under the influence of

## \*Yun-hu Zhang

Male, born in 1987, Ph.D., Associate Professor. His research interests mainly focus on solidification of metals under pulsed electromagnetic fields.

E-mail: zhangyunhu.zyh@163.com

Received: 2017-09-21; Accepted: 2018-01-05

ECP<sup>[13]</sup>. However, ECP is unsuitable for industrial manufacture because the electrodes need to be inserted into the metal melt to conduct electric current through the free surface, which results in the wastage of electrodes and pollution of the metal melt. In addition, it is inconvenient to operate the equipment because the metal melt is electriferous. To overcome the above disadvantages, Gong et al. developed a new technology named pulsed magneto oscillation (PMO) and found that remarkable structure refinement was achievable in commercial pure Al under the influence of PMO<sup>[15]</sup>. Meanwhile, some researchers studied the effects of pulsed magnetic field (PMF) on the solidified structure of various metals. Li and Wang et al. found that PMF can significantly refine the equiaxed grains and reduce the columnar zone in 1Cr18Ni9Ti austenitic stainless steel, and cause the large dendrites in solidified structure of AZ91D alloys to be changed into globular structure<sup>[16, 17]</sup>. Zhang et al. also reported that an electromagnetic field can effectively reduce the macro-segregation due to grain refinement<sup>[18, 19]</sup>. Tu et al. investigated the effect of a low voltage pulse magnetic field (LVPMF) on the shrinkage of pure Al, and the results showed that the depth of shrinkage can be reduced for the great increase of equiaxed grain proportion<sup>[20]</sup>. However, the LVPMF in industry is limited by the high-capacity generator because of its low voltage and the low efficiency.

Pulsed magneto oscillation (PMO) technology has been explored to be used in the solidification process, because it has the following advantages: (a) the alloy melt would not be polluted because of the non-contact with the melt; (b) the pulse generator equipment is relatively simple and has a high electric current output peak; (c) the cost is relatively low due to the small equipment load; (d) the efficiency is high.

Although PMO was frequently applied in a cylindrical ingot with a diameter of only several centimeters, a PMO configuration shown in previous studies<sup>[15,16]</sup> is not suitable for

the production of a heavy ingot (the weight is more than 100 t). In the present work, in order to apply PMO to the production of a heavy ingot, the magnetic coil was located at the hot top of the mould to develop a novel technique named hot-top pulsed magneto oscillation (HPMO). The solidified structure, carbon distribution and compactness of the ingot under the impact of HPMO were systematically investigated at laboratory scale to evaluate the potential industrial application of the HPMO technique.

## 1 Experimental procedures

A schematic view of solidification setup is shown in Fig. 1. In order to simulate the solidification of heavy ingots in industry, a cylindrical steel mould was thermally insulated by floating bead and sand materials with a lateral thickness of 63 mm and bottom thickness of 50 mm to achieve a slow cooling rate which is similar to that in the solidification of heavy ingot of 200–300 t. Multicrystal mullite was chosen as the hot-top thermal insulation material. In addition, in order to simulate the geometry of a heavy ingot, the employed inner size of mould and hot top is  $\Phi 165 \text{ mm} \times 540 \text{ mm}$  and  $\Phi 165 \text{ mm} \times 200 \text{ mm}$ , respectively. A water cooled magnetic coil was located at the hot top to supply PMO by conducting pulsed electric current of 1,400  $K_i$  A, 715  $K_f$  Hz, where  $K_i$  and  $K_f$  are the current peak and discharge frequency parameter of apparatus, respectively. The experimental electromagnetic parameters were chosen based on the simulative experimental results by ANSYS (a commercial simulation software) and were referred to the experimental results of relative low melting point alloys such as Al-Si, Al-Cu and commercial-purity aluminum.

The chemical composition of medium carbon steel is shown in Table 1. The medium carbon steel with a weight of 160 kg was melted and heated up to 1,670 °C in a medium frequency

induction furnace using electromagnetic parameters of 1,000 Hz frequency and 750 V output voltage. Silicon iron, ferromanganese iron, and pure aluminum were added as deoxygenating materials at 1,500 °C. After a holding time of 15 minutes, the melt was poured into the mould through tundish and sprue cup. When the melt was totally filled into the mould, the PMO generator was triggered and then powered off until the ingot was completely solidified. C-type thermocouples protected by  $\text{Al}_2\text{O}_3$  tubing were immersed into the melt through free surface and located at the center of ingot along the axial direction to measure temperature. The measured cooling rate was  $10^{-2} \text{ }^\circ\text{C}\cdot\text{s}^{-1}$ .

The ingot was sectioned longitudinally for metallographic analysis. Five specimens sized at  $42 \text{ mm} \times 20 \text{ mm} \times$

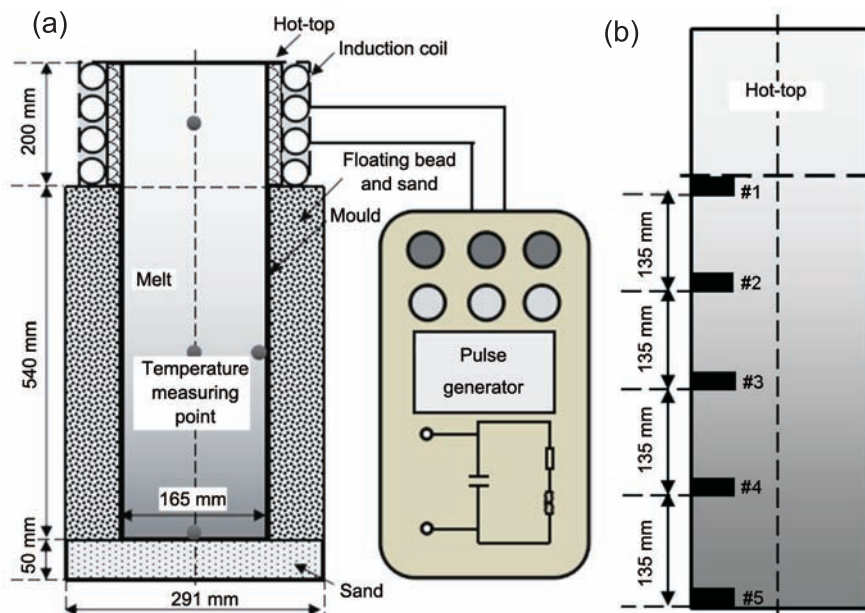


Fig. 1: Schematic views of experimental setup (a) and examined five positions in metallographic specimen (b)



**Table 1: Chemical composition of experimental steel (wt. %)**

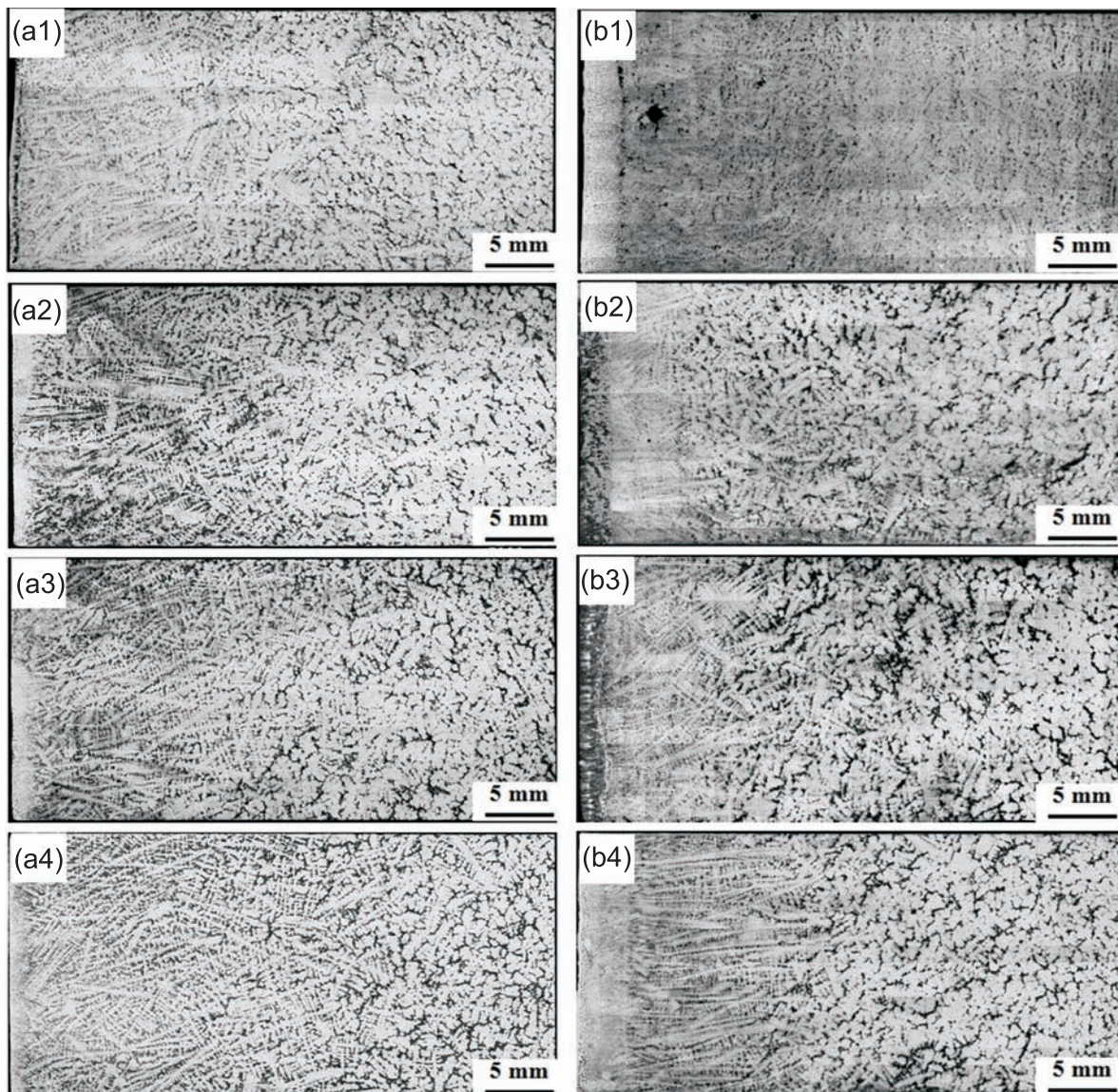
C	Si	Mn	Cr	Ni	Cu
0.42-0.50	0.17-0.37	0.5-0.8	≤0.25	≤0.30	≤0.25

10 mm were selected from one longitudinal section, then ground on SiC paper and polished, then eventually etched in a solution of supersaturating picric acid. The prepared specimens were examined by optical microscope (Imager.A2m, Germany) for microstructure analysis. Carbon segregation distribution and compactness of ingot (except the hot-top part) were measured by LIBSOPA-100 (Laser Induced Breakdown Spectroscopy Original Position metal Analyzer, made by NCS, CISRI, China) in another longitudinal section. The measured area was 82.5 mm × 540 mm. The sample surface was processed by milling machine to get the detective zone, and then the surface was detected by LIBSOPA-100 line by line according to the setup program in the computer to gain the original datum of carbon segregation distribution and compactness of ingot. The carbon segregation distribution and compactness of the ingot was analyzed by the exclusive software finally.

## 2 Results

### 2.1 Solidified structure of ingots without and with HP MO treatment

Figure 2 shows solidified structures of the medium carbon steel. Both columnar and equiaxed structures are observed in the solidified sample produced without the influence of HP MO [Fig. 2(a1-a5)] and the samples (at five positions in Fig. 1b) treated by HP MO [Fig. 2(b1-b5)]. It can be seen that the area of columnar zone was significantly decreased after the treatment of HP MO. In addition, the growth directions of the columnar crystals are almost horizontal in the sample treated by HP MO, whereas the columnar crystals grow not strictly horizontally in the sample without HP MO treatment. Moreover, the solidified structures influenced by HP MO are finer than that without the impact of HP MO. The corresponding measurements were performed to show the variation of the columnar zone, as shown in Fig. 3. The length of the columnar zone of samples at the five positions (Fig. 1b) becomes shorter under the HP MO only except that at the highest position. In particularly, for the columnar zone at the





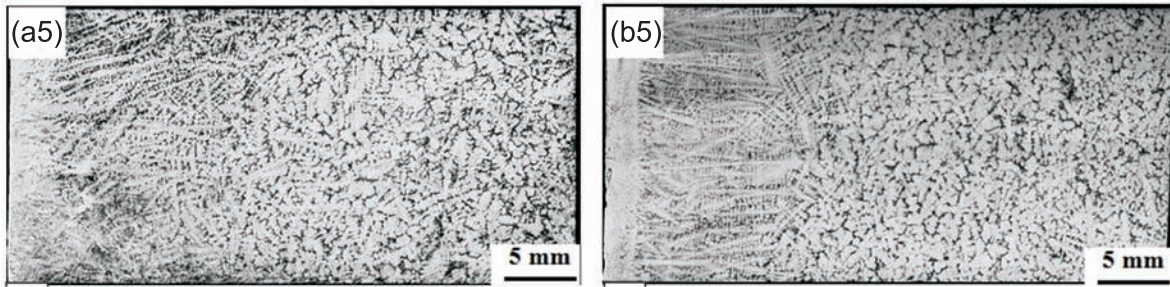


Fig. 2 : Solidified structure of ingots produced without influence of HPMO (a1–a5) and treated by HPMO (b1–b5) (a1–a5 and b1–b5 are corresponding to five positions shown in Fig. 1b, respectively)

three positions (#3, #4 and #5) at the lower part of the ingot, the length is shortened by 24.3%–32.8%.

## 2.2 Carbon segregation and compactness of ingots without and with HPMO treatment

### 2.2.1 Carbon segregation and compactness of untreated ingots

Figure 4 presents the carbon distribution and compactness distribution in the ingot without HPMO treatment. As shown in Fig. 4(a), a serious macro carbon segregation occurred. The positive segregation with a value more than 1.11 can be observed most regions of the upper part of the ingot, while the negative segregation with the lowest value of 0.68 was generated in the lower part of ingot. As shown in the ingot without HPMO (Fig. 4b), the lowest compactness with value less than 0.80 can be observed in the top region of the sample along the center axis, and that at the center of bottom and the 1/2 radius along the axial direction of ingot the value is 0.965 –1.000.

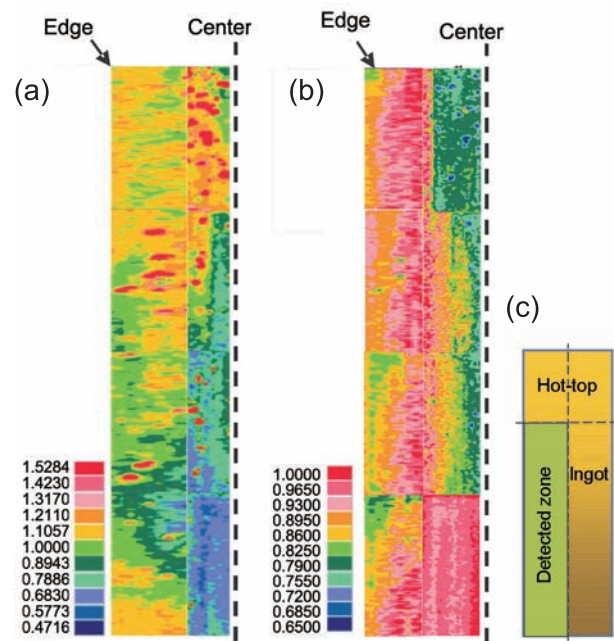


Fig. 4: Contour of carbon distribution (a) and compactness distribution in ingot without HPMO treatment (b), schematic view of detected zone (c)

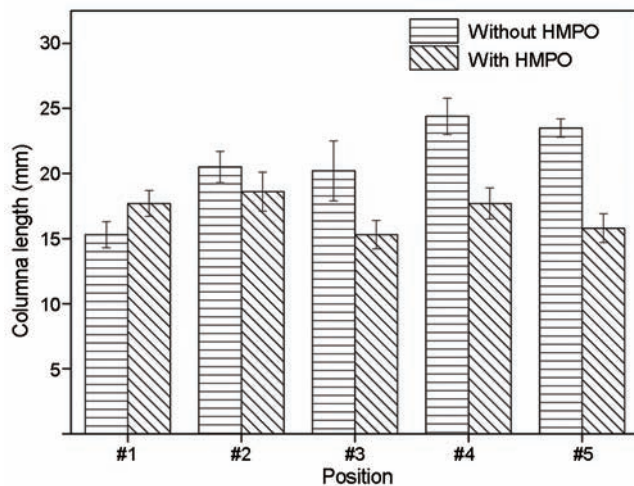


Fig. 3: Columnar length of five positions with and without HPMO treatment

The carbon segregation index  $\Omega$  is given by Eqs. (1) and (2):

$$\Omega = \frac{1}{n} \sum_{i=1}^n |\varepsilon_i - 1| \times 100\% \quad (1)$$

$$\varepsilon_i = \frac{\omega_c^i - \bar{\omega}_c}{\bar{\omega}_c} \quad (2)$$

Where  $\varepsilon_i$  is the carbon segregation of  $i$  position,  $\bar{\omega}_c$  is the average weight percentage of carbon element,  $\omega_c^i$  is the weight percentage of carbon element measured at  $i$  position. The respective carbon segregation indexes along the center axis ( $\Omega_{center}$ ) and the one along edge line ( $\Omega_{edge}$ ) in the ingot without being treated by HPMO were calculated, and the results are shown in Table 2. That  $\Omega_{center}$  is 17.9% and  $\Omega_{edge}$  is 8.7%. The compactness along the center axis ( $C_{center}$ ) is 0.84, along the edge line ( $C_{edge}$ ) is 0.89, and in the entirety ( $C_{entirety}$ ) is 0.86. It can be seen that the compactness along the center axis is lower than that of the edge and entirety.

### 2.2.2 Improvement of carbon segregation and compactness with HPMO treatment

Figure 5 presents the carbon distribution and compactness

Table 2: Carbon segregation and compactness index of ingot without HPMO treatment

	Center axis	Edge line	Entirety
$\Omega$ (%)	17.9	8.7	13.9
$C$	0.8377	0.8876	0.8593



distribution in the ingot with HPMO treatment. The macro-segregation phenomenon became remarkably weak by applying HPMO compared with that in the untreated ingot. It can be found from Fig. 5(a) that the distribution of carbon element become more uniform after being treated by HPMO, the composition in most of the regions is similar with the original composition. In addition, the amplitude of positive or negative segregation is far less than that in the untreated ingot (Fig. 4a). The compactness of the ingot shown in Fig. 5(b) is in the range of 0.93–1.00, which is dramatically enhanced by HPMO. In addition, the homogeneity of the compactness distribution is also improved by HPMO compared with that of the untreated ingot shown in Fig. 4(b).

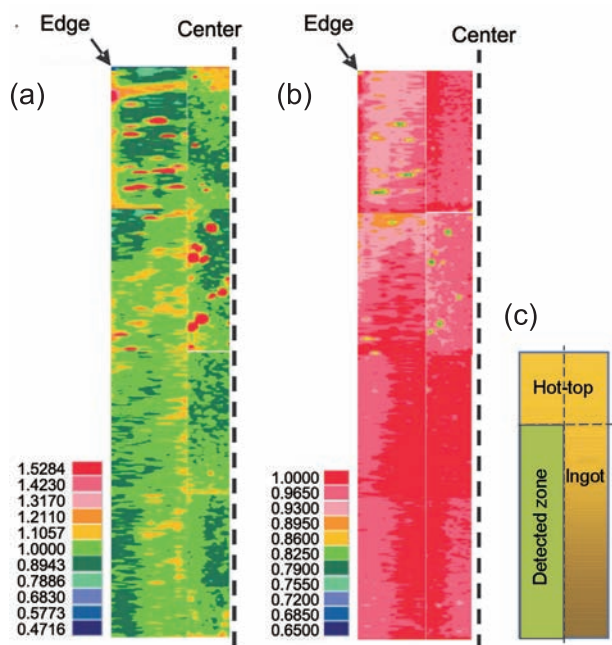


Fig. 5: Contour of carbon distribution (a) and compactness distribution in ingot with HPMO treatment (b), schematic view of detected zone (c)

In order to further show the influence of HPMO on the macro segregation, the respective carbon segregation indices along the center axis ( $\Omega'_{center}$ ), along edge line ( $\Omega'_{edge}$ ) and in the whole section ( $\Omega'_{entirety}$ ) of the treated ingots were calculated, and the results are shown in Table 3. The carbon segregation index at the center in the treated ingot ( $\Omega'_{center}$ ) is 9.7%, which is significantly reduced compared with that in the untreated ingot ( $\Omega_{center} = 17.9\%$ ). This means that the macro segregation in the center zone can be remarkably improved by the applied HPMO. It can be seen that  $\Omega'_{edge}$  is 8.8%, which

Table 3: Carbon segregation index and compactness index of center axis, edge line and entirety of ingot with HPMO treatment

	Center axis	Edge line	Entirety
$\Omega'$ (%)	9.7	8.8	9.1
$C'$	0.9574	0.9426	0.9510

is similar with that in the untreated ingot. It can be said that the segregation index at the edge is almost not influenced by HPMO. In addition, the segregation index from the entire measured section  $\Omega'_{entirety}$  indicates that the homogeneity of carbon element in the whole ingot is promoted after the HPMO, which is obviously decreased from 13.9% in the untreated ingot ( $\Omega_{entirety}$ ) to 9.1% after the HPMO.

In order to clearly show the enhancement of compactness by HPMO, the average compactness indexes along the center axis ( $C'_{center}$ ), edge line ( $C'_{edge}$ ) and in the whole section ( $C'_{entirety}$ ) after being treated by HPMO were calculated, respectively. It can be seen (Table 3) that the compactness along the center axis is slightly higher than that along the edge and in entirety without the HPMO treatment. In these three corresponding calculated results, it can be found that the increment of compactness indexes under the influence of HPMO treatment are higher by 0.12 along the center axis and 0.09 in the entirety than that of untreated ingot. This means that after HPMO treatment, the compactness of the ingot is more uniform than that without HPMO treatment.

### 3 Discussion

#### 3.1 Role of grain refinement

The present work has systematically presented the influence of HPMO on the solidified structure, the solute distribution and the porosities in a cylindrical steel ingot. The present experimental results have shown that the HPMO can significantly improve the solidified structure, weaken the carbon segregation and increase the compactness of ingot. All these influences can be attributed to the HPMO induced grain refinement during the solidification process. In the refined structure, the size decreases and the amount increases markedly for equiaxed grains, so the microstructure is more uniform and compact. As the composition of equiaxed grain is more uniform than columnar, and vast equiaxed grains are heaped up, the carbon distribution can be more uniform and the compactness increased.

As the schematic view shows in Fig. 6, the initial nuclei continuously generated at the hot top of ingot under the HPMO, and then drifted into the bulk melt to prevent the growth of columnar crystal as well as trigger the occurrence of CET. This is the reason why the length of columnar zone is reduced as shown in Figs. 2 and 3.

Moreover, it is well known that the formation of equiaxed grains can

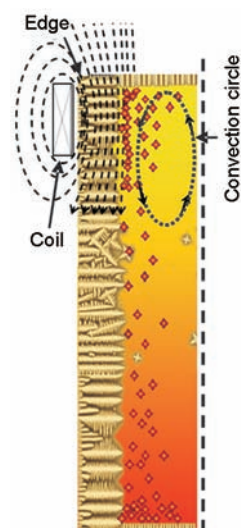


Fig. 6: Schematic view of melt convection and grain moving caused by HPMO

enhance melt feeding to reduce the shrinkage porosities compared with the columnar structure<sup>[11-13]</sup>. In addition, it has been proven that the forced convection can be caused by PMO in the bulk melt. The HPMO induced forced convection can homogenize the temperature field of detected zone, which includes not only the hot top but also the top of the ingot near the hot top. As a consequence, the shrinkage cavity was moved up into the hot top under the HPMO. Hence, the compactness of the ingot was significantly promoted as the measured results show in Fig. 4(b) and Fig. 5(b).

### 3.2 PMO induced electromagnetic fields and their effects

There is no doubt that the generated grain refinement under the HPMO is driven by induced electromagnetic fields. When an electro-pulse passed through the coil, the pulsed magnetic field  $B$  (T) can be produced around the coil and the induced pulsed current  $J$  (A) appeared in the molten metal. According to Faraday electromagnetic induction law, the Lorentz force  $F = J \times B$ , and the direction of Lorentz force is given by the left-hand rule. As a result, the frequently metabolic transient magnetic pressure ( $P$ )<sup>[21]</sup> appears in the melt under the effect of pulsed electromagnetic field, given by Eq. (3).

$$P = \frac{\mu_0 I^2 r^2}{8 \Pi^2 a^4} \quad (3)$$

Where  $P$  (Pa) is transient magnetic pressure,  $I$  (A) is total current passing through the molten metal,  $\mu_0$  ( $\text{N} \cdot \text{A}^{-2}$ ) is vacuum magnetic conductivity,  $r$  (m) is the distance between arbitrary point in molten metal and axis,  $a$  (m) is melt radius. The strength of transient magnetic pressure ( $P$ ) is stronger than that of the melt, so it causes the molten metal oscillation. In the case of skin-layer effect, Lorentz force is created at the certain depth from the side surface to the center of ingot by the coupling effects of the induction current and pulse magnetic field. The direction of the Lorentz force points from the surface to the center of the ingot.

It has been demonstrated that the PMO induced Lorentz force can cause strong forced convection inside the melt of alloys. The numerical simulation and experiments performed by Zhao and Liang<sup>[22-25]</sup> have shown the distribution traits of electromagnetic force and forced convection. As a consequence, PMO has an inevitable effect on the temperature field in the melt. Force convection can eliminate the partial superheat in the center through transporting the superheated melt from center to edge, and decrease the temperature gradient of molten metal. In addition, the electromagnetic force can produce a shrinkage effect to the melt, which makes molten metal pulsate along the axial direction. Under both the effects of forced convection and shrinkage effect, the temperature of the molten metal becomes homogeneous, suppressing the growth of columnar crystals. Meanwhile, the homogeneous temperature field guarantees the survival of formed nuclei. As a result, the number of equiaxed grains increased markedly, and the length of columnar shortened, which contributed to the improvement of the

compactness of the ingot and made the carbon distribution more uniform.

### 3.3 Mechanism of grain refinement driven by PMO

Although intensive researches have been performed to understand the grain refinement mechanism of PMO, it is still unclear until now. Two underlying mechanisms are frequently proposed. One says that the nucleation energy barrier can be reduced by changing the Gibbs free energy under the electromagnetic field in the melt of metal alloys<sup>[26-28]</sup>. The other is that the PMO induced Joule heating, Lorentz force, transient magnetic pressure ( $P$ ), forced convection and other effects can provoke the dendrite fragmentation owing to the dendrite mechanical broken and remelting<sup>[29-35]</sup>. In the solidification process of the melt, the solidified shell with dendrite morphology is firstly frozen against the mould wall. It is possible to cause the temperature and composition fluctuation by the PMO induced pulsed Joule heating, Lorentz force, transient magnetic pressure ( $P$ ) and forced convection to remelt the dendrite arms. As a results, the dendrite pieces are oscillated apart from the solidified shell in the molten melt and drifted into the bottom of ingot (see Fig. 6), called "crystal rain", to generate the finer solidified structure. However, these two possible mechanisms should be clarified by more future studies.

## 4 Conclusions

This work focuses on the solidified structure of a medium carbon steel ingot influenced by HPMO. The results show that the HPMO can cause finer solidified structure to generate, the length of columnar grains to shorten, and the area of equiaxed grain zone to increase. The experimental results confirm that the improved solidified structure mostly profits from the Joule heating effect, forced convection and the grain rain effect under the impact of HPMO treatment. As the result of the HPMO improving solidified structure, the macro segregation and compactness of the ingot are significantly improved. The measured results show not only that the distribution of carbon element in ingot becomes more homogenized, but also that the shrinkage porosity and cavity are significantly reduced. These results mean that the quality of steel ingot can be remarkably improved by the HPMO. The quality improvement is most likely due to the generated grain refinement in the solidified ingot.

The gained knowledge in the present work provides more insights into the solidified steel ingot with large scale under the impact of pulsed electromagnetic field. Since the HPMO induced magnetic field was only performed at the hot top of an ingot, the gained knowledge in the present work provides more insight into the grain refinement driven by PMO compared with the configuration that the whole cylindrical ingot was influenced by PMO. In addition, it has demonstrated that HPMO technology has the potential to be applied in the production of heavy steel ingots to improve the macro-segregation and compactness on an industrial scale. As HPMO



technology has the advantages of non-pollution, low-energy consumption and easy operation, it may play a great role in developing the new technology of improving the ingredient homogeneity in the heavy ingot and promoting the manufacturing level of large-scale equipment. So it can be fully convincing to conclude that HPMO is a potential method to be applied on an industrial scale to promote the quality of a heavy steel ingot.

## References

- [1] Zhao Wenlong, Ma Qingxian. Technological Development of the Forged Low Pressure Rotor of Nuclear Turbine in China. *Applied Mechanics and Materials*. Trans Tech Publications, 2015, 703: 430-435.
- [2] Li Dianzhong, Chen Xingqiu, Fu Paixian, et al. Inclusion flotation-driven channel segregation in solidifying steels. *Nature Communications*, 2014, 5: 1-8.
- [3] Combeau H, Založnik M, Hans S, et al. Prediction of macrosegregation in steel ingots: Influence of the motion and the morphology of equiaxed grains. *Metallurgical and Materials Transactions B*, 2009, 40(3): 289-304.
- [4] Gu J P, Beckermann C. Simulation of convection and macrosegregation in a large steel ingot. *Metallurgical and Materials Transactions A*, 1999, 30(5): 1357-1366.
- [5] Smetana B, Žaludová M, Tkadlečková M, et al. Experimental verification of hematite ingot mould heat capacity and its direct utilisation in simulation of casting process. *Journal of Thermal Analysis and Calorimetry*, 2013, 112(1): 473-480.
- [6] Heidarzadeh M, Keshmiri H. Influence of mould and insulation design on soundness of tool steel ingot by numerical simulation. *Journal of Iron and Steel Research, International*, 2013, 20(7): 78-83.
- [7] Liu Xinbao, Osawa Y, Takamori S, et al. Grain refinement of AZ91 alloy by introducing ultrasonic vibration during solidification. *Materials Letters*, 2008, 62(17): 2872-2875.
- [8] Watanabe T, Shiroki M, Yanagisawa A, et al. Improvement of mechanical properties of ferritic stainless steel weld metal by ultrasonic vibration. *Journal of Materials Processing Technology*, 2010, 210(12): 1646-1651.
- [9] Bode O, Schwerdtfeger K, Geck H G, et al. Influence of casting parameters on void volume and centre segregation in continuously cast 100Cr6 blooms. *Ironmaking & Steelmaking*, 2008, 35(2): 137-145.
- [10] Ludlow V, Normanton A, Anderson A, et al. Strategy to minimise central segregation in high carbon steel grades during billet casting. *Ironmaking & Steelmaking*, 2005, 32(1): 68-74.
- [11] Ahmadein M, Wu M, Ludwig A. Analysis of macrosegregation formation and columnar-to-equiaxed transition during solidification of Al-4 wt.% Cu ingot using a 5-phase model. *Journal of Crystal Growth*, 2015, 417: 65-74.
- [12] Malekan M, Shabestari S G. Effect of grain refinement on the dendrite coherency point during solidification of the A319 aluminum alloy. *Metallurgical and Materials Transactions A*, 2009, 40(13): 3196.
- [13] Ma Jianhong, Li Jie, Gao Yulai, et al. Improving the carbon macrosegregation in high-carbon steel by an electric current pulse. *Metals and Materials International*, 2009, 15(4): 603-608.
- [14] Liao Xiliang, Zhai Qijie, Luo Jun, et al. Refining mechanism of the electric current pulse on the solidification structure of pure aluminum. *Acta Materialia*, 2007, 55(9): 3103-3109.
- [15] Gong Yongyong, Luo Jun, Jing Jinxian, et al. Structure refinement of pure aluminum by pulse magneto-oscillation. *Materials Science and Engineering: A*, 2008, 497(1): 147-152.
- [16] Li Qiushu, Song Changjiang, Li Huigai, et al. Effect of pulsed magnetic field on microstructure of 1Cr18Ni9Ti austenitic stainless steel. *Materials Science and Engineering: A*, 2007, 466(1): 101-105.
- [17] Wang Bin, Yang Yuansheng, Zhou Jixue, et al. Microstructure refinement of AZ91D alloy solidified with pulsed magnetic field. *Transactions of Nonferrous Metals Society of China*, 2008, 18(3): 536-540.
- [18] Zhang Beiji, Cui Jianzhong, Lu Guimin, et al. Effect of electromagnetic field on the macrosegregation of continuous casting 7075 alloy. *Transactions of Nonferrous Metals Society of China*, 2003, 13(1): 158-161.
- [19] Zhang Beiji, Cui Jianzhong, Lu Guimin, et al. Effect of frequency on the microstructure of electromagnetic field casting 7075 alloy. *Acta Metallurgica Sinica*, 2002, 38(2): 215-215. (In Chinese)
- [20] Tu Xurong, Zhou Quan, Chen Leping. Effect of low-voltage pulsed magnetic field on solidification structure and shrinkage of pure aluminum. *Hot Working Technology*, 2010, 39(3): 43-45. (In Chinese)
- [21] Yan Hongchun, He Guanhu, Zhou Benlian, et al. The influence of electric discharging current on the solidified structure of Sn-10%Pb alloy. *Acta Metallurgica Sinica*, 1997, 33(4): 352-358. (In Chinese)
- [22] Zhao Jing, Yu Jihao, Li Qiushu, et al. Structure of slowly solidified 30Cr2Ni4MoV casting with surface pulsed magneto-oscillation. *Materials Science and Technology*, 2015, 31(13): 1589-1594.
- [23] Zhao Jing, Cheng Yufeng, Han Ke, et al. Numerical and experimental studies of surface-pulsed magneto-oscillation on solidification. *Journal of Materials Processing Technology*, 2016, 229: 286-293.
- [24] Liang Dong, Liang Zhuyuan, Zhai Qijie, et al. Nucleation and grain formation of pure Al under Pulsed Magneto-Oscillation treatment. *Materials Letters*, 2014, 130: 48-50.
- [25] Liang Dong, Liang Zhuyuan, Sun Jie, et al. Grain refinement of commercial pure Al treated by Pulsed Magneto-Oscillation on the top surface of melt. *China Foundry*, 2015, 12(1): 48-53.
- [26] Qin Rongshan, Bhowmik A. Computational thermodynamics in electric current metallurgy. *Materials Science and Technology*, 2015, 31(13): 1560-1563.
- [27] Qin Rongshan, Zhou Benlian. Effect of electric current pulses on grain size in castings. *International Journal of Non-Equilibrium Processing (UK)*, 1998, 11(1): 77-86.
- [28] Qin Rongshan. Critical assessment 8: outstanding issues in electropulsing processing. *Materials Science and Technology*, 2015, 31(2): 203-206.
- [29] Wang Ping, Lu Guimin, Cui Jianzhong. Microstructure of nearby liquidus semi-continuous casting aluminum alloy A356. *Acta Metallurgica Sinica*. 2002, 38(4): 389-392.
- [30] Li Qiushu, Li Haibin, Zhai Qijie. Structure evolution and solidification behavior of austenitic stainless steel in pulsed magnetic field. *Journal of Iron and Steel Research International*, 2006, 13(5): 69-72.
- [31] Guo Shijie, Cui Jianzhong, Le Qichi, et al. The effect of alternating magnetic field on the process of semi-continuous casting for AZ91D billets. *Material Letters* 2005, 59: 1841-1844.
- [32] Hellawell A, Liu Shan, Lu Shuzu. Dendrite fragmentation and the effects of fluid flow in castings. *Journal of the Minerals, Metals and Materials Society*, 1997, 49(3): 18-20.
- [33] Wang Bin, Yang Yuansheng, Ma Xiaoping, et al. Simulation of electromagnetic-flow fields in Mg melt under pulsed magnetic field. *Transactions of Nonferrous Metals Society of China*, 2010, 20: 283-288.
- [34] Li Yingju, Yang Yuansheng. Grain refinement of as-cast super alloy IN718 under action of low voltage pulsed magnetic field. *Transactions of Nonferrous Metals Society of China*, 2011, 21(6): 1277-1282.
- [35] Edry I, Frage N, Hayun S. The effect of pulse magneto-oscillation treatment on the structure of aluminum solidified under controlled convection. *Materials Letters*, 2016, 182: 118-120.

This study was financially supported by the National Natural Science Foundation of China (Granted No. U1760204, 51504048) and the National Key Research Program of China (Granted No. 2017YFB0701800).